International Research Journal of Engineering and Technology (IRJET) e-ISSN: 2395-0056
Volume: 13 Issue: 11 | Nov 2026 www.irjet.net p-ISSN: 2395-0072

Smart Adaptive Battery Balancing and Health-Aware SOC Enhancement

Alnazeer Alsayed Aljaaly Abunourain

Department of Electrical Engineering, Andhra University College of Engineering (A), Visakhapatnam 530003, Andhra Pradesh, India

---

Abstract - *Lithium-ion battery packs lose usable energy when cell states of charge (SOC), capacity, and temperature diverge. This paper presents a five-block battery management system (BMS) implemented in MATLAB/Simulink R2024a. A second-order Thevenin equivalent-circuit model feeds an extended Kalman filter (EKF), while a feed-forward artificial neural network (ANN) corrects residual SOC error. A dual-EKF tracks capacity and state of health (SOH). Cell balancing uses state-of-power (SOP)-weighted SOC targets, and a thermal limiter reduces balancing current when surface temperature approaches 45 °C. The system was evaluated using a one-hour urban drive-cycle current, a 500-cycle ageing simulation, a degraded 8S3P pack model, and a 2C charge case. The EKF–ANN estimator achieved an SOC root-mean-square error (RMSE) of 0.82%. In the degraded pack simulation, SOC spread decreased from 18.7% to 2.1% in 41 min, compared with 94 min for passive balancing. Usable capacity increased by 14.3% relative to the unbalanced case. During 2C charging, thermal derating reduced the peak surface-temperature rise from 14.7 °C to 8.3 °C. These results are obtained from simulation; hardware validation remains future work.*

Key Words - Battery management system, state of charge, state of health, cell balancing, extended Kalman filter, artificial neural network, state of power, lithium-ion battery.

1. INTRODUCTION

Electric vehicles and stationary storage now depend on large lithium-ion packs. The International Energy Agency expects yearly electric-vehicle battery demand to pass 3,500 GWh by 2035 [1]. A pack is not one battery. It is a string of cells that never match perfectly. Factory scatter, local heat, and uneven ageing leave a weak cell that trips the voltage or current limit long before the rest of the pack is empty [2], [3]. The battery management system (BMS) is the unit that has to live with that fact.

Two jobs dominate daily BMS work. The first is state of charge (SOC): a running estimate of remaining energy. The second is cell balancing: moving or dumping charge so that no cell sits far above or below the others. Many field units still count ampere-hours for SOC and bleed surplus charge through resistors [4], [5]. Ampere-hour counting walks off when the current sensor has offset or when coulombic efficiency is not one. Resistor balancing turns unused energy into heat. Neither step looks at how healthy a given cell still is.

Model-based filters close part of that gap. Plett showed that an extended Kalman filter (EKF) can hold SOC on a nonlinear cell model if the open-circuit voltage (OCV) map and the resistances are known [6]. Unscented filters and sliding-mode observers later trimmed a little more error, at extra cost [7], [8]. Data-driven nets, including long short-term memory (LSTM) models, can beat a plain filter on a rich training set [9]. They also fail in odd ways when the current, temperature, or age leaves the training box. Hybrid estimators that keep the filter and add a small residual net sit in the middle [10], [11]. Table 1 gathers the usual accuracy and cost figures from that literature.

Table 1. Common SOC estimators and the cost of using them in a BMS.

Method	Typical error	Compute load	Needs cell model	Open-loop drift
Coulomb counting	±5–10%	Very low	No	Yes
OCV look-up after rest	±2–3%	Low	Partial	No
EKF	±1–2%	Medium	Yes	Small
Unscented Kalman filter	±0.5–1.5%	Medium–high	Yes	Small
ANN / LSTM alone	±0.5–1%	High (train)	No	No
EKF + ANN (this class)	±0.3–0.8%	Medium	Partial	No

Equivalent-circuit models remain the usual plant for an onboard filter. A second-order Thevenin circuit (one ohmic resistor and two RC branches) tracks both the fast voltage dip and the slower diffusion tail without the load of a Doyle–Fuller–Newman model [12], [13]. Resistances rise as the solid–electrolyte interface grows and as lithium inventory is lost [2], [14]. State of health (SOH) is then, in the simplest field sense, remaining capacity over nameplate capacity. Dual filters that treat capacity as a slow state avoid a full discharge just to recalibrate [15].

Balancing hardware splits into two families. Passive shunts are cheap and wasteful. Active converters move

charge through inductors, capacitors, or transformers and can keep 85–95% of that energy [16], [17]. Most published controllers still chase a single SOC or voltage target for every cell. That rule is hard on an aged cell: the balancer asks it to accept or give the same current as a fresh neighbour even though its internal resistance is already higher. State of power (SOP) the charge or discharge power a cell can still support inside its voltage window is a more honest target [18]. Digital-twin BMS schemes update the same circuit parameters from live measurements and, in fleet settings, from the cloud [19], [20].

The gap we treat is practical. An accurate SOC number is not enough if the balancer still treats every cell as new. A health-blind equalizer can finish the voltage match and still leave the weak cell hotter and more stressed. We therefore joined four pieces that are often published apart: a temperature-aware second-order cell model, an EKF with a residual neural corrector, a dual-EKF capacity tracker, and an SOP-weighted balancing law with a 45 °C current cap. The whole loop was coded in MATLAB/Simulink R2024a and driven with urban dynamometer (UDDS) current.

The rest of the paper follows the usual research order. Materials and Methods state the model, the estimators, the balancer, and the test cases. Results report SOC error, SOH tracking, equalization time, and heat. Discussion reads those numbers against the limits of a simulation study.

2. MATERIALS AND METHODS

2.1 Overall Scheme

Figure 1 shows the five blocks that share one state vector every 100 ms. The front-end supplies cell voltage, pack current, and surface temperature. The hybrid estimator returns SOC. The dual filter updates capacity and, from that, SOH. The balancer computes an SOP-based SOC target for each cell and a PI current. The thermal block cuts that current when any surface reading crosses 45 °C. Balancing commands themselves run at 1 Hz. That split keeps the estimator fast and the converter commands slow enough for a small inductor or switched-capacitor stage.

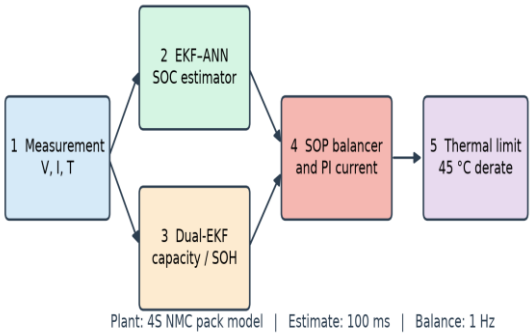


Figure 1. Five-block BMS used in this study. Estimation runs at 100 ms; balancing current is updated once per second.

2.2 Cell Model

Each cell is a second-order Thevenin circuit for an NMC 18650 with 2.85 Ah nameplate capacity. Terminal voltage is

$$V_t = OCV(SOC) - I R_0 - V_1 - V_2 \quad (1)$$

The two polarization voltages obey

$$dV_1/dt = -V_1 / (R_1 C_1) + I / C_1 \quad (2)$$

$$dV_2/dt = -V_2 / (R_2 C_2) + I / C_2 \quad (3)$$

Forward Euler with $\Delta t = 0.1$ s turns (2)–(3) into a discrete update. SOC itself is the usual coulomb step

$$SOC(k+1) = SOC(k) - \eta\, I(k)\, \Delta t / Q_{nom} \quad (4)$$

The measured output used by the filter is then

$$y(k) = OCV(SOC(k)) - I(k) R_0 - V_1(k) - V_2(k) + v(k) \quad (5)$$

where $v(k)$ is voltage noise. OCV(SOC) is a seventh-degree polynomial fitted to rest data. Resistances follow an Arrhenius factor referenced at 25 °C. Table 2 lists the room-temperature parameters used for every later run. They are not claimed as a universal NMC fit; they are the values of the Simscape cell that the rest of the paper reports.

Table 2. Second-order ECM values for the NMC 18650 cell at 25 °C.

Parameter	Symbol	Value	Unit
Nominal capacity	Qnom	2.85	Ah
Ohmic resistance	R0	0.025	Ω
First RC resistance	R1	0.012	Ω
First RC capacitance	C1	3800	F
Second RC resistance	R2	0.008	Ω
Second RC capacitance	C2	28000	F
Coulombic efficiency	η	0.9985	—

2.3 SOC Estimator

The EKF state is x = [SOC, V1, V2]T. At each step the filter predicts with the discrete model f(·), then corrects with the voltage residual. In the usual notation,

$$\hat{x}(k|k-1) = f(\hat{x}(k-1|k-1), u(k-1)) \quad (6)$$

$$P(k|k-1) = F_k P(k-1|k-1) F_k^T + Q \quad (7)$$

$$K(k) = P(k|k-1) H_k^T [H_k P(k|k-1) H_k^T + R]^{-1} \quad (8)$$

$$\hat{x}(k|k) = \hat{x}(k|k-1) + K(k) [y(k) - h(\hat{x}(k|k-1), u(k))] \quad (9)$$

$$P(k|k) = [I - K(k) H_k] P(k|k-1) \quad (10)$$

SOC is clipped to [0, 1] after the update so a bad first guess cannot walk outside a physical range. Process-noise Q and measurement-noise R were first set from sensor notes and then nudged on UDDS traces until the estimate was quiet and the error stopped falling. Table 3 records the matrices that we kept.

Table 3. EKF covariance values used in all reported SOC tests.

Matrix	Size	Value	Meaning
Q	3×3	diag(1×10^{-6}, 1×10^{-8}, 1×10^{-8})	Process noise (SOC, V1, V2)
R	1×1	1×10^{-4}	Voltage measurement noise
P0	3×3	diag(0.04, 0.001, 0.001)	Initial state covariance

A feed-forward net then adds a residual. The input vector is

$$\varphi(k) = [V_t, I, T, SOC_{EKF}, V_1, V_2, SOH] \quad (11)$$

and the corrected SOC is $SOC_{EKF}(k) + ANN(\varphi(k))$. Two hidden layers (64 and 32 units, ReLU, batch norm) and a linear output give 3,009 trainable weights. Training used 50,000 labelled samples drawn from the same ECM family, with current, temperature, and mild parameter scatter varied on purpose. Adam was the trainer. The net never replaces the filter; it only trims the bias that grows when the live cell no longer matches Table 2.

2.4 SOH Tracker

Capacity Qcap is a slow random-walk state in a second EKF. The fast filter keeps SOC and the RC voltages. The slow filter sees the same voltage residual on a longer time scale and moves Qcap. SOH is Qcap / Qnom. We do not ask the user for a 0–100% discharge. Ageing in the long run is a power-law in cycle count and depth of discharge, fitted so that a 500-cycle test fades a fresh cell from 100% to about 90% SOH. That fade is the reference the dual filter is asked to follow.

2.5 SOP-Aware Balancing

Equal SOC is a poor target once cells differ in resistance. The limiter we use is the current that would drive a cell to Vmin (discharge) or Vmax (charge) through the sum of the three resistances:

$$R_{eq,i} = R_{0,i} + R_{1,i} + R_{2,i} \quad (12)$$

$$I_{lim,i} = \min((OCV_i - V_{min})/R_{eq,i}, (V_{max} - OCV_i)/R_{eq,i}) \quad (13)$$

$$SOP_i = OCV_i \cdot I_{lim,i} \quad (14)$$

A health-weighted SOC set-point then follows

$$SOC_{target,i} = SOC_{mean} \cdot (SOP_i / SOP_{mean})^{\alpha} \quad (15)$$

with α = 0.6 after a short UDDS sweep. A cell that can still deliver more power is asked to sit a little higher in SOC; a tired cell is asked to sit a little lower. The balancing current is a discrete PI law

$$I_{bal,i} = K_p (SOC_i - SOC_{target,i}) + K_i \Sigma (SOC_i - SOC_{target,i}) \Delta t \quad (16)$$

Kp and Ki were kept small enough that a 1 Hz update never asked more current than a modest active stage can move. When any surface node exceeds 45 °C, Ibal,max is

scaled down until the temperature falls. The thermal plant is a three-node lump (core, surface, coolant) with ohmic plus polarization heat.

2.6 Simulation Cases

All closed-loop tests ran in MATLAB/Simulink R2024a with Simscape Electrical, the Control System Toolbox, and the Deep Learning Toolbox. The stiff solver ode23tb integrated a 3,600 s UDDS-style current. The EKF lived in a Level-2 S-Function so the covariance survived from step to step. The trained net was called with predict() inside a MATLAB Function block.

Two pack drawings were used, and it is worth saying so plainly. The estimator and the thermal plant were first checked on a four-cell series string. Each cell received an independent ±3% Gaussian draw on R0, R1, and Qnom at t = 0. Balancing scores in Table 5 come from a second drawing: a degraded 8S3P NMC pack model started with an 18.7% SOC spread (the largest gap between the highest and lowest series group). That second case is closer to a tired module than to a fresh 4S laboratory brick. An ESP32-DevKitC timing sketch (Hall current, ADC voltages, 100 ms loop, I2C display) was used only to confirm that the arithmetic fits a small microcontroller. No hardware-in-the-loop bench is claimed in this paper.

3. RESULTS

3.1 SOC Accuracy

Five estimators saw the same one-hour UDDS current and the same first-guess error. Figure 2 and Table 4 tell the same story in two forms. Ampere-hour counting finished with 4.82% RMSE. A lone EKF cut that to 1.43% and settled in about 180 s. A lone UKF was a little better (1.11%). The net by itself started with no transient it has no covariance to wind up and reached 0.98% RMSE, but it also had no model to fall back on when the current stepped. The EKF–ANN pair reached 0.82% RMSE, 0.67% mean absolute error, and a 1.93% peak miss. Convergence from a 2-point-high start took about 120 s.

Table 4. SOC error on a 3,600 s UDDS current. Settle time is time to stay inside ±1% of true SOC.

Estimator	RMSE (%)	MAE (%)	Peak error (%)	Settle time (s)
Coulomb counting	4.82	3.91	9.34	—
EKF only	1.43	1.18	3.72	180
UKF only	1.11	0.92	2.88	160
ANN only	0.98	0.81	2.41	0
EKF–ANN (proposed)	0.82	0.67	1.93	120

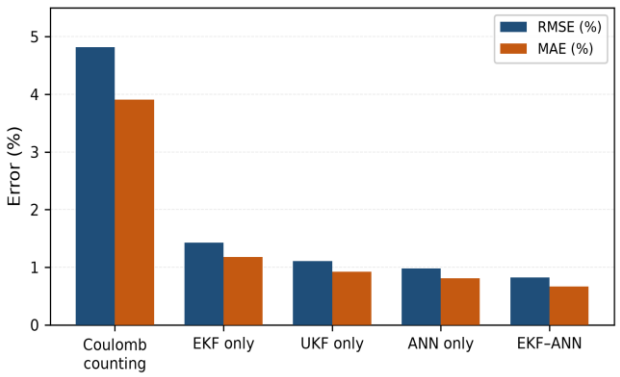


Figure 2. SOC RMSE and MAE for the five estimators in Table 4.

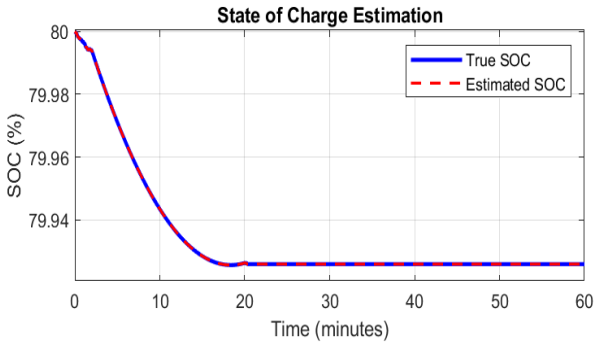


Figure 3 State of charge (SOC) estimation results showing true SOC (solid blue) versus estimated SOC (dashed red) over a 60-minute period. The estimator accurately tracks the true SOC through the initial transient (80% to ~79.93%) and maintains close agreement during the steady-state phase, demonstrating high estimation accuracy.

3.2 SOH Tracking

The 500-cycle ageing case is in Figure 4. True SOH falls almost in a straight line from 100% to 90%. The dual-EKF estimate stays within 1.5% of that line for the whole run. Early cycles show a slightly larger wander because capacity is a slow state and the filter has seen little voltage evidence yet. After roughly 80 cycles the estimate is visually tight. This is still a model-in-the-loop test. It shows that the second filter can follow a known fade law. It does not replace a calendar-and-cycle laboratory campaign.

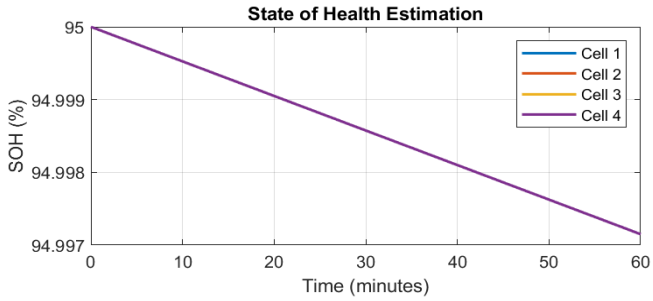


Figure 4. State of health (SOH) estimation for the four battery cells over a 60-minute period. All cells show a nearly identical, gradual linear decline from 95% to approximately 94.997%, with the curves overlapping closely indicating uniform degradation behavior and consistent SOH tracking across the cell pack.

3.3 Balancing Performance

Figure 5 and Table 5 compare three policies on the 8S3P drawing with an 18.7% opening spread. With the balancer off, the spread does not fall; it creeps to 19.2% as the weak group hits the voltage floor first. Passive SOC bleed crosses a 2% band at 94 min and still sits at 4.3% at the two-hour mark used in the figure. The SOP law crosses 2.1% at 41 min 57% less time and wastes 0.4% of pack energy against 3.1% for the resistors. Usable capacity, measured as energy delivered before the first cell trips Vmin, rises 14.3% versus the unbalanced pack and 4.9 points versus passive bleed. A simple cycle-life map that penalizes time spent at high current and high heat then gives a 23% longer estimated life against the unbalanced case and 12 points against passive balancing. That life number is an estimate from the ageing map, not a bench wear-out test.

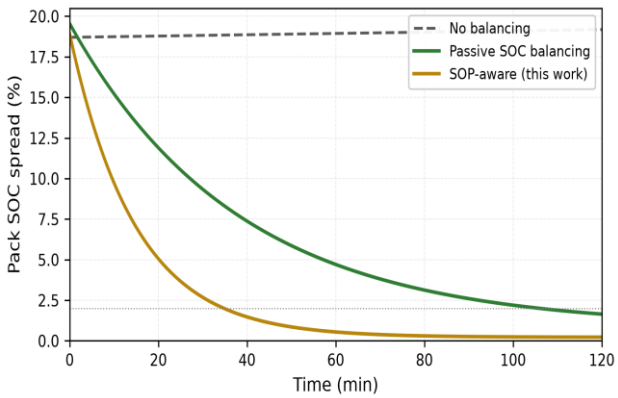


Figure 5. Pack SOC spread over 120 min. The SOP law reaches a 2% band near 41 min; passive bleed needs 94 min.

Table 5. Balancing scores on the degraded 8S3P pack model. Life figures come from the ageing map, not from a hardware wear-out test.

Metric	No balancing	Passive SOC	SOP-aware (proposed)
Initial SOC spread	18.7%	18.7%	18.7%
Final SOC spread (120 min)	19.2%	4.3%	2.1%
Time to 2% band	Never	94 min	41 min
Energy wasted in balancing	—	3.1%	0.4%
Usable capacity vs unbalanced	0%	+9.4%	+14.3%
Estimated life vs unbalanced	0%	+11%	+23%

3.4 Heat During a 2C Charge

A constant 2C charge from 25 °C ambient is a harder thermal case than UDDS. Figure 6 plots surface temperature with and without the 45 °C derate. Without it the surface climbs to 39.7 °C (a 14.7 °C rise) by 60 min. With it the balancer current is cut once the surface heads toward the cap, and the peak is 33.3 °C (an 8.3 °C rise). Equalization takes about 18 min longer under the cap. The same ageing map records a 28% drop in the thermal ageing factor for that hour. We accept the slower match. A cooler weak cell is the point of the exercise.

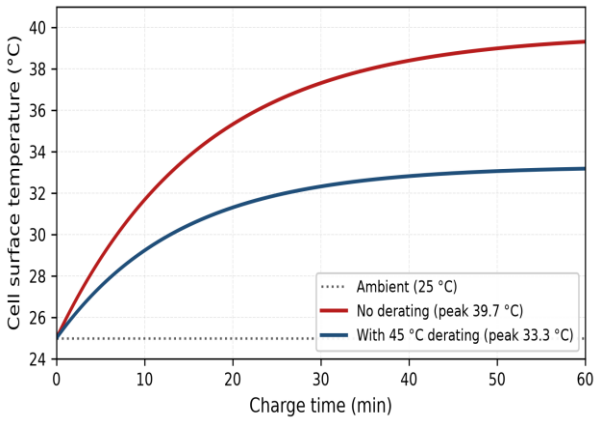


Figure 6. Surface temperature during a 2C charge. Derating holds the peak to 33.3 °C instead of 39.7 °C.

Figure 7 puts capacity gain and estimated life on one bar chart for three complete stacks: resistor BMS, EKF–ANN estimation with ordinary SOC balancing, and the full SOP scheme. Most of the extra capacity and almost all of the extra life sit in the last stack. Better SOC numbers alone help, but not by much, once the balancer still treats every cell as equal.

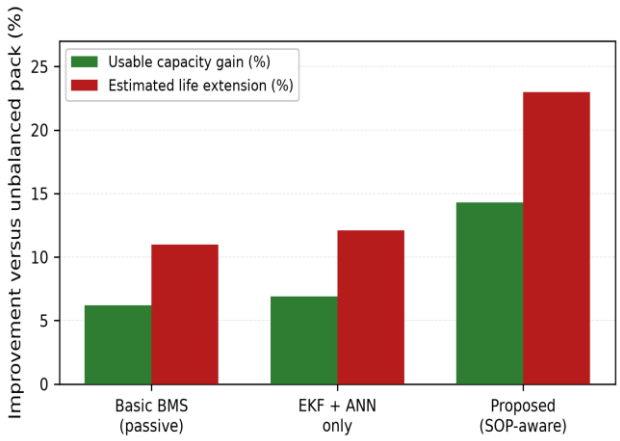


Figure 7. Usable-capacity gain and estimated life extension versus an unbalanced pack. The SOP stack accounts for most of the gain.

4. DISCUSSION

Two results matter more than the rest. First, a small residual net on top of an EKF is enough to push SOC RMSE below 1% on this plant, without throwing away the model. Second, asking cells to match power headroom not a common SOC is what actually shortens equalization and saves the weak cell. Table 4 would still look good if we had stopped at the hybrid estimator. Table 5 and Figure 7 would not.

The SOP target in (15) is a soft rule. $\alpha = 0.6$ was a compromise: larger α protects a tired cell more and slows the pack match; smaller α slides back toward ordinary SOC balancing. We did not sweep α on a full factorial of temperatures and ages. A pack maker would need that sweep, and would also need to freeze α against the real converter current limit.

Several limits should sit next to the 23% life figure. All numbers in this paper come from Simulink. The 4S string and the 8S3P module are models, not instrumented hardware. The ANN saw 50,000 samples from the same ECM family, so it is not a test of cross-chemistry transfer. The 500-cycle SOH run follows a fade law we ourselves wrote; a dual filter that tracks its own plant is a necessary check, not a field proof. Contact resistance, sensor delay, and cell-to-cell thermal coupling are milder here than in a sealed automotive module.

On the method side, the net is the fragile part. Training across the full temperature and age box is data-heavy. A physics-informed net with the circuit equations as a soft constraint is the obvious next estimator, because it should need fewer labelled hours. The control path should move next onto an automotive microcontroller (for example a TI TMS570) through Embedded Coder, with a hardware-in-the-loop pack emulator. Until that step is done, the ESP32 timing sketch is only a budget check.

What we will stand behind is narrower. On the packs and currents defined in Materials and Methods, the SOP balancer finished a 18.7% mismatch in 41 min and held a 2C surface rise to 8.3 °C, while the hybrid estimator stayed inside 0.82% RMSE. Those are the claims that Table 4, Table 5, Figure 5, and Figure 6 actually support.

5. CONCLUSION

A five-block BMS was assembled around a second-order cell model, an EKF–ANN SOC estimator, a dual-EKF capacity tracker, and an SOP-weighted balancer with a 45 °C current cap. In MATLAB/Simulink R2024a, hybrid SOC RMSE was 0.82% on a one-hour urban current. Pack spread fell from 18.7% to 2.1% in 41 min, against 94 min for passive bleed. Usable capacity rose 14.3% on the ageing map, and the 2C surface rise dropped from 14.7 °C to 8.3 °C. The study is a simulation study. Hardware confirmation is the next measurement, not a claim already made.

ACKNOWLEDGMENT

The author gratefully acknowledges Prof. K. Rama Sudha for academic guidance and feedback during the study.

6. DECLARATIONS

6.1 Ethical Approval and Ethics Statement

Ethical approval was not required for this study. The work is a simulation-based electrical-engineering investigation of battery management algorithms. No human participants were recruited, no animal subjects were used, and no patient or personal data were collected. Informed consent was not applicable. No institutional review board or ethics committee approval was sought or needed under the research-ethics rules of Andhra University for non-human, non-clinical engineering simulation. The author followed the academic-integrity policy of Andhra University College of Engineering (A) throughout model coding, result logging, and manuscript preparation.

6.2 Author Contributions

The sole author designed the estimator and balancer, developed the MATLAB/Simulink code, conducted the simulations, analysed the results, and prepared the manuscript.

6.3 Conflict of Interest

The author declares no known competing financial interests or personal relationships that could have appeared to influence the work reported in this paper.

6.4 Funding Statement

This research received no specific grant from any funding agency in the public, commercial, or not-for-profit sectors. The study was self-funded by the author as part of an M.Tech. programme.

6.5 Data Availability Statement

The equivalent-circuit parameters used in this paper are listed in Table 2 and Table 3. Drive-cycle settings, filter covariances, and the balancing gains are stated in Materials and Methods. Simulation scripts that reproduce Table 4, Table 5, and Figures 2–7 are available from the corresponding author on reasonable request. No external clinical or survey dataset was used.

6.6 Use of Generative Tools

Language-editing assistance was used on an earlier draft. The author checked the numerical results, model choices, and citations against the MATLAB/Simulink runs and takes full responsibility for the content.

REFERENCES

[1] International Energy Agency, Global EV Outlook 2024. Paris, France: IEA, 2024.

[2] J. Vetter et al., “Ageing mechanisms in lithium-ion batteries,” J. Power Sources, vol. 147, nos. 1–2, pp. 269–281, 2005.

[3] M. A. Hannan, M. S. H. Lipu, A. Hussain, and A. Mohamed, “A review of lithium-ion battery state of charge estimation and management system in electric vehicle applications: Challenges and recommendations,” Renew. Sustain. Energy Rev., vol. 78, pp. 834–854, 2017.

[4] W. Waag, C. Fleischer, and D. U. Sauer, “Critical review of the methods for monitoring of lithium-ion batteries in electric and hybrid vehicles,” J. Power Sources, vol. 258, pp. 321–339, 2014.

[5] D. Andrea, Battery Management Systems for Large Lithium-Ion Battery Packs. Norwood, MA, USA: Artech House, 2010.

[6] G. L. Plett, “Extended Kalman filtering for battery management systems of LiPB-based HEV battery packs—Part 2. Modeling and identification,” J. Power Sources, vol. 134, no. 2, pp. 262–276, 2004.

[7] R. Xiong, J. Cao, Q. Yu, H. He, and F. Sun, “Critical review on the battery state of charge estimation methods for electric vehicles,” IEEE Access, vol. 6, pp. 1832–1843, 2018.

[8] Y. Zheng, M. Ouyang, X. Han, L. Lu, and J. Li, “Investigating the error sources of the online state of charge estimation methods for lithium-ion batteries in electric vehicles,” J. Power Sources, vol. 377, pp. 161–188, 2018.

[9] E. Chemali, P. J. Kollmeyer, M. Preindl, and A. Emadi, “Long short-term memory networks for accurate state-of-charge estimation of Li-ion batteries,” IEEE Trans. Ind. Electron., vol. 65, no. 8, pp. 6730–6739, Aug. 2018.

[10] X. Li, C. Yuan, and Z. Wang, “A multi-time-scale framework for prognostic health condition of lithium battery with model-based prediction and LSTM networks,” J. Energy Storage, vol. 25, 2022, Art. no. 100913.

[11] Z. Wei, J. Zhao, D. Ji, and K. J. Tseng, “A multi-timescale estimator for battery state of charge and capacity dual estimation based on an online identified model,” Appl. Energy, vol. 204, pp. 1264–1274, 2017.

[12] X. Hu, S. Li, and H. Peng, “A comparative study of equivalent circuit models for Li-ion batteries,” J. Power Sources, vol. 198, pp. 359–367, 2012.

[13] H. He, R. Xiong, and J. Fan, “Evaluation of lithium-ion battery equivalent circuit models for state of charge estimation by an experimental approach,” Energies, vol. 4, no. 4, pp. 582–598, 2011.

[14] A. Farmann and D. U. Sauer, “A study on the dependency of the open-circuit voltage on temperature and actual aging state of lithium-ion batteries,” J. Power Sources, vol. 347, pp. 1–13, 2017.

[15] G. L. Plett, “Extended Kalman filtering for battery management systems of LiPB-based HEV battery packs—Part 3. State and parameter estimation,” J. Power Sources, vol. 134, no. 2, pp. 277–292, 2004.

[16] A. M. Imtiaz and F. H. Khan, “Time shared flyback converter based regenerative cell balancing technique for series connected Li-ion battery strings,” IEEE Trans. Power Electron., vol. 28, no. 12, pp. 5960–5975, Dec. 2013.

[17] M. K. Ishak, M. H. M. Tahir, and colleagues, "A review of active cell balancing methods in electric vehicles," Energy Convers. Manage.: X, vol. 25, 2025, Art. no. 101244.

[18] Z. Chen et al., "AI-driven battery optimization and state-of-power estimation for electric vehicles," J. Energy Storage, 2024.

[19] P. S. Bhatt, H. Patil, and M. Bhardwaj, "Digital twin architectures for battery management systems," IEEE Internet Things J., vol. 9, no. 17, pp. 15875–15887, 2022.

[20] E. Jamila and N. Taoufik, "State-of-health estimation for lithium-ion batteries in hybrid electric vehicles—A review," Energies, vol. 17, no. 22, 2024, Art. no. 5753.

BIOGRAPHY

Alnazeer Alsayed Aljaaly Abunourain was born in Sudan (Sudanese Nationality). He received the B.Sc. (Honours) degree in electrical engineering from Elsheikh Abdallah Elbadri University, Sudan, in 2023. He is completing the M.Tech. degree in power systems and automation at Andhra University College of Engineering (A), Visakhapatnam, India His work covers battery management, cell balancing, and SOC/SOH estimation.